

ORIGINAL RESEARCH

Non-invasive monitoring of tomato graft dynamics using thermography and fluorescence quantum yields measurements

 Carlos Frey  | Andrés Hernández-Barriuso | Antonio Encina  | José Luis Acebes 

Área de Fisiología Vegetal. Departamento de Ingeniería y Ciencias Agrarias, Facultad de Ciencias Biológicas y Ambientales, Universidad de León, León, Spain

Correspondence

Antonio Encina and José Luis Acebes, Área de Fisiología Vegetal. Departamento de Ingeniería y Ciencias Agrarias. Facultad de Ciencias Biológicas y Ambientales, Universidad de León, León, Spain.

Email: a.encina@unileon.es and jl.acebes@unileon.es

Funding information

Ministerio de Ciencia, Innovación y Universidades, Grant/Award Number: FPU18/04934; Universidad de León

Edited by Y. Utsumi

Abstract

Grafting involves a sequence of modifications that may vary according to genotypes, grafting techniques and growing conditions. This process is often monitored using destructive methods, precluding the possibility of monitoring the entire process in the same grafted plant. The aim of this study was to test the effectiveness of two non-invasive methods—thermographic inference of transpiration and determination of chlorophyll quantum yields—for monitoring graft dynamics in tomato (*Solanum lycopersicum* L.) autografts and to compare the results with other reliable measures: mechanical resistance parameters and xylem water potential. The mechanical resistance of grafted plants steadily increased from 6 days after grafting (DAG), 4.90 ± 0.57 N/mm, to reach values similar to non-grafted plants at 16 DAG, 8.40 ± 1.78 N/mm. Water potential showed an early decrease (from -0.34 ± 0.16 MPa in non-grafted plants to -0.88 ± 0.07 MPa at 2 DAG), recovering at 4 DAG to reach pre-grafting values at 12–16 DAG. Thermographic inference of transpiration dynamics displayed comparable changes. Monitoring maximum and effective quantum yield in functional grafts showed a comparable pattern: an initial decline, followed by recovery from 6 DAG onwards. Correlation analyses revealed a significant correlation between variation in temperature (thermographic monitoring of transpiration), water potential ($r = 0.87$; $p = 0.02$) and maximum tensile force ($r = 0.75$; $p = 0.05$). Additionally, we found a significant correlation between maximum quantum yield and some mechanical parameters. In conclusion, thermography monitoring, and to a lesser extent maximum quantum yield measurements, accurately depict changes in key parameters in grafted plants and serve as potential timing indicators of graft regeneration, rendering them valuable tools for monitoring graft functionality.

1 | INTRODUCTION

Plant grafting is an ancient horticultural technique in which two living plant parts, the stem (scion) and roots (rootstock), are joined

together in such a way that vascular continuity is established between the two partners, resulting in a single plant (Hartmann et al., 2018; Figure 1A). Generally, the goal is to obtain a new chimera plant to increase yield, reduce susceptibility to diseases and increase tolerance to biotic and abiotic stresses (Colla et al., 2010; Louws et al., 2010).

Carlos Frey and Andrés Hernández-Barriuso contributed equally to this work.

This is an open access article under the terms of the [Creative Commons Attribution-NonCommercial-NoDerivs](https://creativecommons.org/licenses/by-nc-nd/4.0/) License, which permits use and distribution in any medium, provided the original work is properly cited, the use is non-commercial and no modifications or adaptations are made.

© 2023 The Authors. *Physiologia Plantarum* published by John Wiley & Sons Ltd on behalf of Scandinavian Plant Physiology Society.

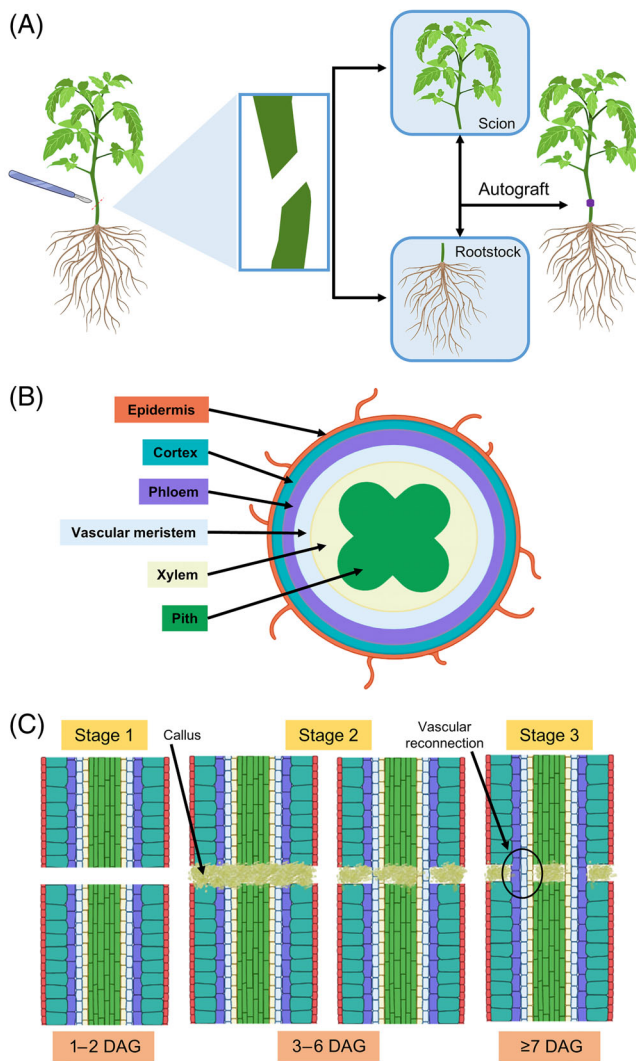


FIGURE 1 (A) Scheme of grafting. In the case of autografts, scion and rootstock belong to the same plant. (B) Schematic transversal section of a tomato stem. (C) Schematic longitudinal sections of the graft healing process in the three stages (Stage 1: cut and wound response; Stage 2: callus proliferation and vasculature development; Stage 3: vascular reconnection consolidated). Approximate temporal scales (in days after grafting; DAG) are provided at the bottom of the scheme.

Nowadays, fruit-bearing Solanaceae are commercially grafted on a large scale (Bletsos & Olympios, 2008). Tomatoes are among the most widely grown and consumed vegetables. In 2021, a total amount of more than 5 million ha was sown worldwide, with a production of more than 189 million tonnes of tomatoes, according to the FAO (2021). The increasing use of grafting techniques in tomato crops helps to manage various types of diseases and, hence increasing yield, reducing dependence on agrochemicals and providing an eco-friendly alternative for these purposes (Oda et al., 2005).

The formation of the graft union is a dynamic and continuous phenomenon involving a complex series of events at the physiological, cellular and molecular levels that are necessary to ensure the successful union between rootstock and scion (Fernández-García et al., 2004;

Frey et al., 2022, 2023; Melnyk et al., 2015). In addition, grafting is an important research tool for understanding how different physiological mechanisms are coordinated in a wide range of plants (Notaguchi et al., 2020; Reeves et al., 2022).

Three main stages can be identified during the development of tomato grafts (Figure 1B, C) (Cui et al., 2021; Melnyk et al., 2015; Moore, 1984). Briefly, in the first stage, corresponding to an early damage response, initial callus formation occurs in the graft union zone, coupled with the proliferation of callus cells on the cut surfaces of the scion and rootstock (Jeffrey & Yeoman, 1983; Pina & Errea, 2005). Occasionally, defensive responses of cell walls at the cut edges may prevent scion-rootstock attachment during this stage (Frey et al., 2021). In the second phase, the callus cells related to the vascular meristem, phloem and xylem parenchyma differentiate first, forming the xylem and then the initial part of the phloem, and stem re-vascularisation begins (Hartmann et al., 2018). Finally, new vascular tissues develop, providing complete reconnection and revascularisation in the graft zone. This allows the sap to flow between the scion and the rootstock, leading to full recovery of the functionality of the grafted plant (Fan et al., 2015; Melnyk, 2017).

The lack of vascular continuity between the scion and the rootstock impairs water, nutrient and photosynthate transport along the stem, damaging the physiological status of the scion and rootstock. To achieve complete graft healing, the graft must overcome the stresses caused by this separation and repair the stem tissues. To this end, a series of complex molecular and structural processes are activated in both the scion and the rootstock, including enzyme expression, the production of stress-related compounds, accumulation, depletion and/or translocation of phytohormones, cell dedifferentiation and vascular tissue differentiation. The success of the graft mainly depends on the plant's efficiency during these processes (Martínez-Ballesta et al., 2010).

The graft healing process can fail at various stages; when this occurs, it is important to identify it as soon as possible in order to take early action and try to solve the problems detected. Moreover, the actual duration of the different stages varies considerably according to genotypes, growth conditions and grafting methodology; therefore, the implementation of methods for monitoring the grafting process may help to improve the efficiency of the technique.

Frequently used methods for monitoring graft development include measuring growth parameters (plant height, stem diameter, fresh and dry weight of above-ground part and/or under-ground part and root-shoot ratio) (Sun et al., 2021), (bio)chemical composition (mineral nutrients, sugars, vitamin C and pigments, such as chlorophyll and carotenoids) (Sun et al., 2021), fruit yield and quality (hardness, soluble solid, soluble sugar, titratable acid, vitamin C and lycopene), physiological markers (such as stomatal conductance) (Gosa et al., 2022) and even physical parameters (such as electrical resistance) (Yang et al., 1993), anatomical studies of connecting xylem elements (e.g., Melnyk et al., 2015; Thomas et al., 2022) or the use of mobile dyes (e.g. Melnyk et al., 2015; Zhang et al., 2022). However, most of these methods are invasive or even destructive, and therefore unsuitable for following up the graft process on individual plants.

Hence, it is desirable to develop methods that are non-invasive, simple, cost-effective, fast and capable of monitoring a large number of plants. Two potentially useful techniques for monitoring the dynamics of grafting are infrared thermography and the measurement of chlorophyll quantum yields.

Infrared thermography is a widely used imaging technique for analysing plant interactions with the environment (Jones, 2004). It is based on thermographic camera detecting the heat emitted by the objects under study and subsequent analyse of these data to estimate temperature variations. The loss of vascular continuity in the grafted plant alters water transport along the stem and thus reduces transpiration. In consequence, heat dissipation from the leaf surface is restricted and hardly any temperature difference will be detected between the leaves and the environment. As vascular continuity is restored, transpiration and, thus, heat dissipation increase, leading to a reduction in leaf temperature relative to the environment (Costa et al., 2013; Savvides et al., 2022; Torii et al., 1992). Thermography has been suggested as a technique to assess the quality of the graft union (Torii et al., 1992), but this would require overcoming several technical difficulties (Savvides et al., 2022).

Meanwhile, chlorophyll fluorescence is a good indicator of light-dependent photosynthetic processes, and measurements of this feature are widely established in plant-environment studies. Two chlorophyll fluorescence parameters are usually obtained: maximum quantum yield, corresponding to photosystem II photochemistry, and effective quantum yield of non-photochemical processes in photosystem II (Roháček, 2002). Potentially, any stress that impairs the photosynthetic machinery will reduce quantum yield efficiency. Consequently, the effects of scion stresses due to grafting and recovery from these can potentially result in changes in maximum and/or effective quantum yield, which can be measured using a chlorophyll fluorometer (Mauro et al., 2020).

The aim of this study was to test the effectiveness of these two minimally invasive methods (thermography and maximum and effective quantum yield measurements) for potential use in monitoring graft dynamics, using tomato autografts as a model system and seeking the maximum success rate. These methods will be compared with other single-point measurements related to graft healing, such as mechanical resistance and xylem water potential. It is expected that the results obtained will provide the basis for selecting potential early markers of grafting success, which could serve as reliable and useful tools for grafting operators.

2 | MATERIALS AND METHODS

2.1 | Plant material

Tomato (*Solanum lycopersicum* 'Minibel', Mascarell Semillas S.L.) seeds were pre-germinated on a wet filter paper for 24 h. The resulting seedlings were individually grown in 200 mL containers containing a black peat-perlite substrate (1:1) and placed in a growth chamber at $24 \pm 1^\circ\text{C}$ under light ($40 \mu\text{mol m}^{-2} \text{s}^{-1}$) with 16/8 photoperiodic conditions and

over 50% relative humidity. The substrate was irrigated every 3 days with full Hoagland solution (Hoagland & Arnon, 1938) to approximately 100% of field capacity throughout the experiment.

2.2 | Autografting method

When the plant stems were 4–5 mm in diameter (about 1-month-old), a splice graft was performed 5–10 mm below the cotyledonary leaves: scion and rootstock from the same plant were joined and fixed by a graft clip (Toogoo®). After grafting, plants were placed in a healing chamber at $24 \pm 1^\circ\text{C}$ to maintain high relative humidity and reduce wilting in the first few days. Illuminance and relative humidity were regulated during grafting healing, as described in Table S1, using shade cloths and water vaporisation, respectively.

2.3 | Mechanical resistance evaluation

A universal tensile testing system (Servosis, ME-402) was used to determine the evolution of mechanical resistance in the stems of five tomato grafts per DAG throughout the grafting process. The strength was quantified by measuring the maximum force (N) necessary to split apart the graft union. The remaining mechanical resistance parameters (maximum elastic tensile force, yield point, coefficient of tightness and extent of breakage) were measured simultaneously during the assays using the universal tensile testing system. To prevent the stem from tearing, plastic plugs were placed at the ends of the stem and tightly adhered using quick-drying epoxy paste (Ultraglue, Fischer).

2.4 | Xylem water potential measurement

Xylem water potential of scions was measured throughout the grafting process using a Scholander pressure chamber (model 600, PMS Instrument Co.). The measurements were carried out by cutting the stem at the internode between the third and fourth leaf of five plants per DAG.

2.5 | Determination of stem xylem hydraulic conductance

The stem xylem hydraulic conductance at the grafting point was assessed in five grafted plants per DAG using a methodology proposed by Melcher et al. (2012). Briefly, a 2 cm stem segment containing the attachment zone was sampled, fitted to the lower end of a 50 cm vertical silicon tube and connected above with a 50 mL final reservoir filled with distilled water (total water column height was 60.5 cm), taking care to avoid air bubbles. The pressure exerted by the water column ($5.9 \cdot 10^{-3}$ MPa) provided a flow of water passing from the scion through the rootstock, which was collected at the lower end of the segment in a tube and weighed at intervals until

detecting a linear response as a function of time. The equation used to determine conductance was: $K' = Q/\Delta P$, where ΔP is the pressure and Q is the mass flow rate. $\Delta P = \rho gh$, where ρ is water density; g is gravitational acceleration; and h is water column height.

2.6 | Thermal imaging

Twenty plants were used to infer leaf transpiration dynamics using a thermographic camera (C3, FLIR-MSX) vertically positioned 30 cm above each plant. The emissivity value was set at 0.95 (Jones, 2004; Savvides et al., 2022). The plants were taken out of the healing chamber and placed on a laboratory workbench close to the culture chamber. Thermal images were captured under controlled conditions ($22 \pm 1.5^\circ\text{C}$; $41\% \pm 2\%$ relative humidity) at the same hour in the afternoon. Similar room temperature and vapour pressure were maintained for all days and imaging times. No air flow was detected in the laboratory. Thermographic images (RBG) were analysed using the FLIR Tools programme, taking three measurements of the surface at room temperature and three measurements of the apical leaflets of the last three developed leaves for each plant. The measure points were circles with a 5-pixel radius. The temperature value of these points was considered the average among all the pixels in the circle. Changes in transpiration for each DAG were inferred from the difference between environmental temperature and plant temperature (Δ temperature).

2.7 | Measurement of chlorophyll quantum yields

To assess photosystem II efficiency, chlorophyll quantum yields were measured using a pulse-amplitude modulated chlorophyll fluorometer (PAM-210, Heinz Walz GmbH). Quantum yield was measured on the three apical leaflets of three mature leaves per plant. The plants were taken out of the healing chamber but kept in the culture chamber for measurements. Controlled conditions ($25 \pm 1^\circ\text{C}$; $57.5\% \pm 7.5\%$ relative humidity) were maintained for all days and measuring times. Measurements were taken in the morning, at the same time each day. Thirty plants were used per DAG to determine maximum quantum yield, and all measurements were carried out after plant darkness adaptation. To ensure effective quantum yield measurement, the same 30 plants were maintained for at least 2 h under light conditions ($40 \mu\text{mol m}^{-2} \text{s}^{-1}$).

2.8 | Stereomicroscopy techniques

Free-hand transverse sections of the tomato graft junction were obtained and stained with phloroglucinol (showing lignin) to identify the xylem to compare its distribution with maximum tensile force evolution. These samples corresponded to grafts used in the mechanical resistance assay. Other free-hand transverse sections were obtained ≈ 5 mm above the graft union and stained with methylene blue dye solution. This dye was used to stain the functional vessels by forcing the dye through the graft union from the rootstock to the scion by applying negative pressure with a syringe prior to cutting. These

samples corresponded to grafts used in the stem xylem hydraulic conductance assay and were taken to visualise the functional vasculature for comparison with the xylem conductance data. Both types of free-hand sections were observed using a stereomicroscope Nikon SMZ1500 equipped with a camera Nikon D4.

2.9 | Statistical analyses

To ascertain the existence of any statistically significant differences, the Shapiro–Wilk and Levene tests were performed to, respectively, determine normal distribution and homoscedasticity. Extreme values (outliers) in Figures 2 and 3 were removed for the statistical analysis. One-way ANOVA was then performed, followed by Tukey's HSD post hoc test, to determine statistical significance. Pearson's linear correlation analysis was also performed. The significance level in both cases was set at p -value ≤ 0.05 . Detection of statistically significant differences and multivariate Principal Component Analysis (PCA) was performed using the Rstudio software package (1.4.1106-©-2009–2021 RStudio, PBC). Pearson's linear correlation analysis was performed using IBM SPSS Statistics v. 25.0.

3 | RESULTS

3.1 | Progression of mechanical resistance during grafting

The mean values for graft tensile strength (maximum tensile force) between the scion and the rootstock became measurable after 6 DAG (until then, they were not sufficiently adhered), yielding a value of 4.9 ± 0.57 N/mm, which steadily increased throughout the graft healing period, although significant differences between 6 and 12 DAG were not detected due to high variability (Figure 4A). However, after 16 DAG, the maximum tensile force was 8.4 ± 1.78 N/mm, and no significant differences in maximum tensile force were found when compared to non-grafted plants, showing an almost complete recovery of adhesion strength.

Other mechanical resistance parameters—maximum elastic tensile force, yield point, coefficient of tightness and extent of breakage—were also evaluated (Figure S1). The extent of breakage and the yield point remained below the values of non-grafted plants. However, the maximum elastic tensile force and the coefficient of tightness showed a similar pattern to that of the maximum tensile force, reaching the values of non-grafted controls at 16 DAG. Transversal sections of non-grafted stems and split grafts showed the development of the vasculature at the graft junction. A clear xylem ring (highlighted in red by phloroglucinol staining for lignin) became visible at 16 DAG (Figure 4B).

3.2 | Evolution of water potential during graft healing

An early, rapid and significant decrease in xylem water potential was measured in the scions after grafting (from -0.34 ± 0.16 MPa on non-grafted plants to -0.88 ± 0.07 MPa at 2 DAG; Figure 5). At

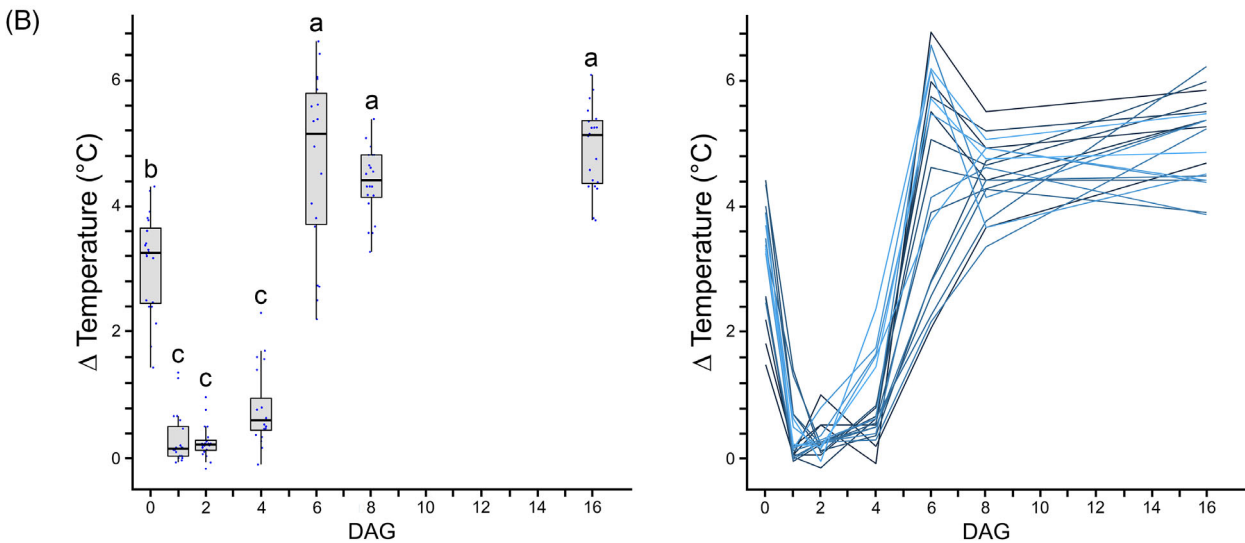
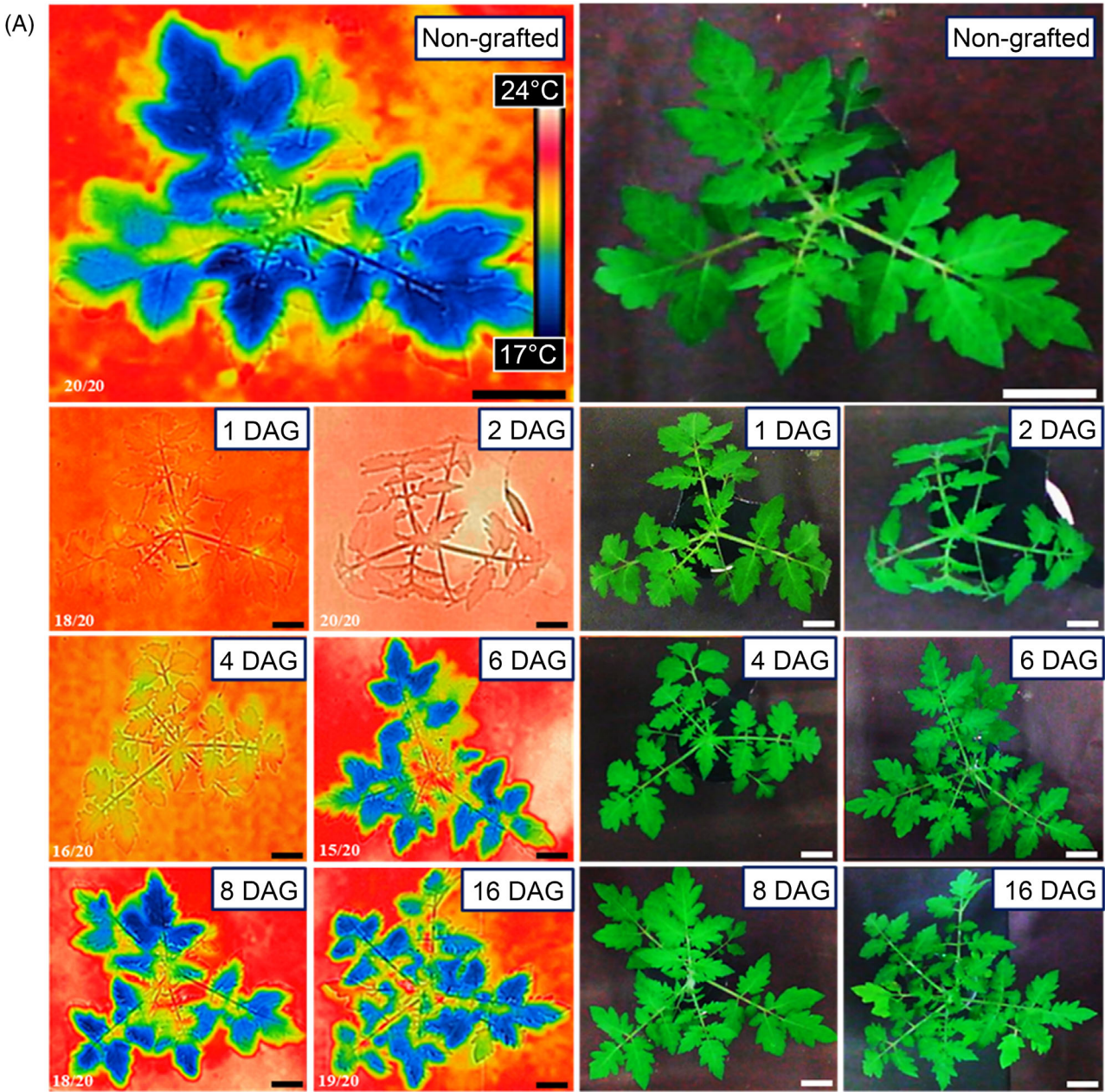


FIGURE 2 Legend on next page.

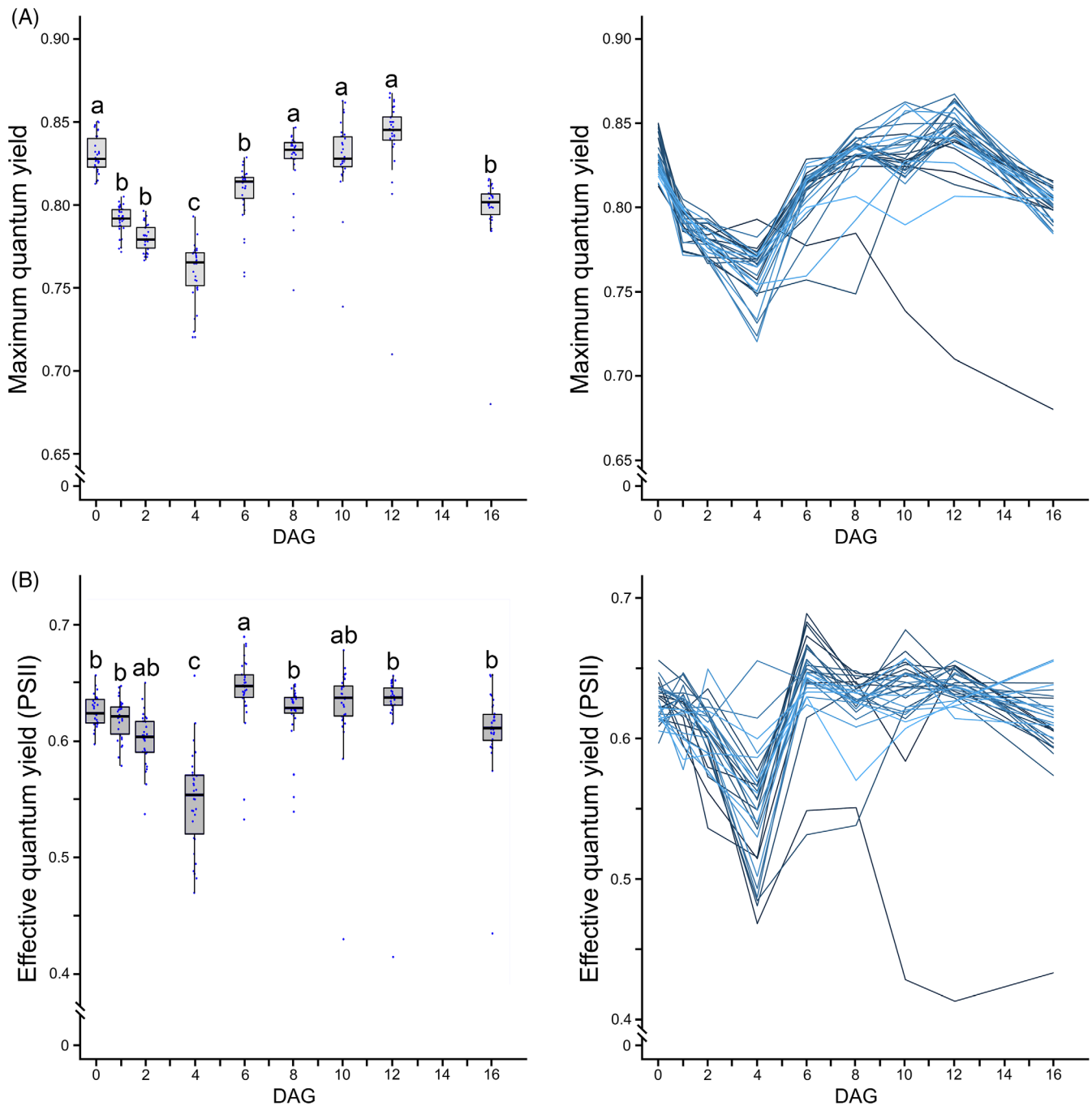
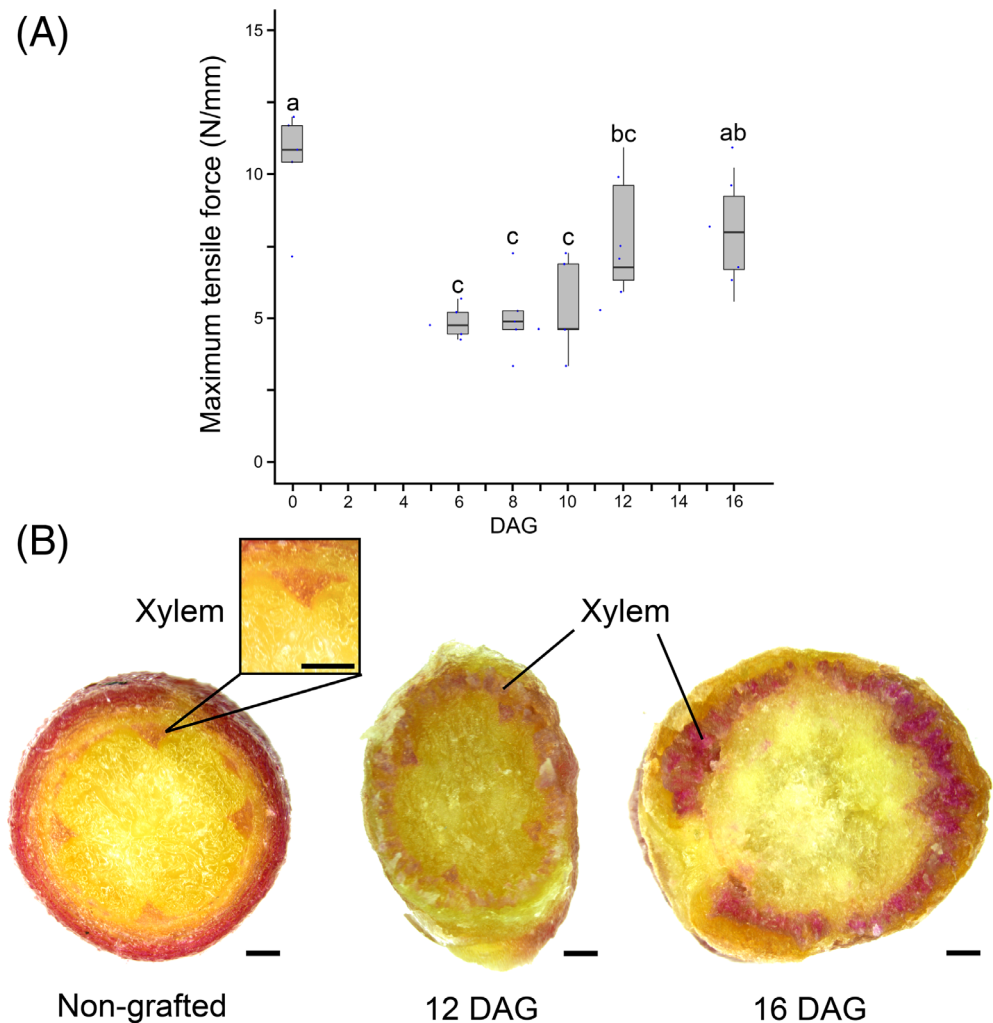


FIGURE 3 Variation in maximum and effective quantum yield of 30 plants throughout the grafting process. (A) Box plot representation of maximum quantum yield as a function of time after grafting (left side); time-dependent changes in maximum quantum yield of the individual plants measured as before (right side). (B) Box plot representation of effective quantum yield (PSII) as a function of time after grafting (left side); time-dependent changes in effective quantum yield of the 30 individual plants measured as before (right side). In box plots, different letters indicate significant differences at the p -value ≤ 0.05 level after ANOVA analysis of variance followed by Tukey's test. 0 DAG indicates non-grafted plants at the beginning of the experiment.

FIGURE 2 (A) Left side: infrared thermography top views of representative plants on different days after grafting. The colour palette for temperatures ranges from red (high temperatures) to blue (low temperatures). The ratio $(X/20)$ at the bottom left of each image indicates the number of plants with the same phenotype as the representative image. Scale bars: 5 cm. Right side: same representative plants under natural lighting. (B) Left side: box plot representation of time-dependent changes in inferred transpiration as variation in temperature (ambient T - leaf T) throughout the grafting process ($n = 20$). Right side: variation in inferred transpiration of the 20 individual plants as shown before. In box plots, different letters indicate significant differences at the p -value ≤ 0.05 level after ANOVA analysis of variance followed by Tukey's test. 0 DAG indicates non-grafted plants at the beginning of the experiment.

FIGURE 4 (A) Box plot representation of the variation in graft tensile strength (maximum tensile force), relativized to the diameter of the section, throughout the grafting process ($n = 5$). Measurements at 1, 2 and 4 days after grafting (DAG) could not be performed because the grafts were not sufficiently adhered. Different letters indicate significant differences at the p -value ≤ 0.05 level after ANOVA analysis of variance followed by Tukey's test. 0 DAG indicates non-grafted plants at the beginning of the experiment. (B) Magnified observation of phloroglucinol staining of non-grafted and graft transversal sections at 12 and 16 DAG. Bar = 1 mm.



8 DAG, the recovery of xylem water potential to the levels measured in non-grafted plants was well advanced. However, this parameter was only fully restored at later stages (12 and 16 DAG). To determine the reconstitution of the water column, xylem water conductance was also evaluated (Figure S2). Xylem functionality was detected at 4 DAG but was still very low, and it was not until 16 DAG that it reached values close to those of the non-grafted plants (Figure S2). The increase in water conductance during grafting was concurrent with the development of functional vascular connections that reconnected flow through the xylem. The functional vasculature of the scion at 4 DAG only occurred in small patches, whereas at 16 DAG larger areas of functional vasculature, forming a ring was evident (Figure S2).

3.3 | Monitoring of graft healing dynamics by non-invasive methods

3.3.1 | Transpiration inference by thermography

By measuring the temperature at the leaf surface of scions, it is possible to infer transpiration dynamics under controlled conditions,

such as the absence of wind or any other fluctuating weather conditions. This minimises the effect of variability derived from factors such as variations in air vapour pressure deficit, differences in plant leaf surfaces or even changes in the orientation of the sampled leaves (Maes & Steppe, 2012; Costa et al., 2013). It is, therefore, appropriate to use plants cultivated in growth chambers with controlled environmental variables (Savvides et al., 2022). In our study, infrared thermal images showed clear changes in leaf temperature (Figure 2A) and, therefore, in inferred transpiration during graft healing.

Differences between ambient and leaf temperature decreased significantly on the first DAG until reaching almost zero values (no temperature difference with respect to a surface at room temperature). Thereafter, the inferred transpiration gradually recovered from 4 DAG onwards. Although the values recorded were highly variable, the grafted plants recovered their pre-cutting transpiration values by 6 DAG, with no further changes occurring throughout the grafting process (Figure 2B). Monitoring the transpiration of each individual plant revealed a consistent general pattern despite the variability observed among the individual grafted plants (Figure 2B).

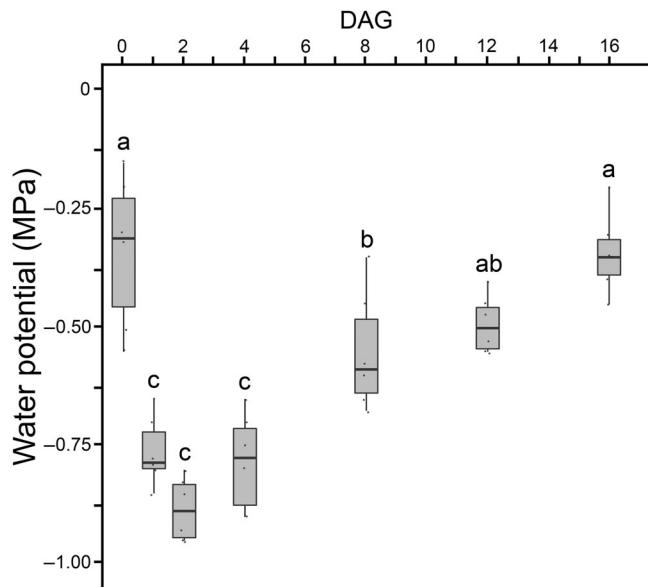


FIGURE 5 Box plot representation of the variation in water potential of scions throughout the grafting process ($n = 5$). Different letters indicate significant differences at the p -value ≤ 0.05 level after ANOVA analysis of variance followed by Tukey's test. DAG: days after grafting. 0 DAG indicates non-grafted plants at the beginning of the experiment.

3.3.2 | Quantum yield measurements

The maximum quantum yield of photosystem II underwent a significant sharp decline soon after grafting (1–4 DAG) but subsequently increased so that there was no further significant difference compared to non-grafted plants by 8 DAG (Figure 3A). The evolution of the effective quantum yield (Figure 3B) mimicked the above parameter with slight differences, as the drop in effective quantum yield was delayed (4 DAG vs. 1 DAG for maximum quantum yield) and recovered more quickly; from 6 DAG onwards, grafted plants had similar values compared to non-grafted controls.

Interestingly, some grafted plants that had shown a significant decrease in both maximum and effective quantum yield at 6–8 DAG showed no difference thereafter and finally proved to be successfully developed grafts. Nevertheless, it was possible to follow the evolution of one unfunctional graft that had shown significantly lower maximum and effective quantum yield values as early as 6 DAG and did not recover thereafter (Figure 3).

3.4 | Variable correlation and multivariate analysis

Pearson's linear correlation test identified significant correlations among mechanical resistance parameters, water potential, temperature difference (ΔT), maximum quantum yield and effective quantum yield. In particular, ΔT correlated significantly with maximum tensile force ($r = 0.75$; $p = 0.05$) and water potential ($r = 0.87$; $p = 0.02$; Figure 6). In addition, maximum quantum yield correlated significantly with all mechanical resistance parameters except maximum elastic

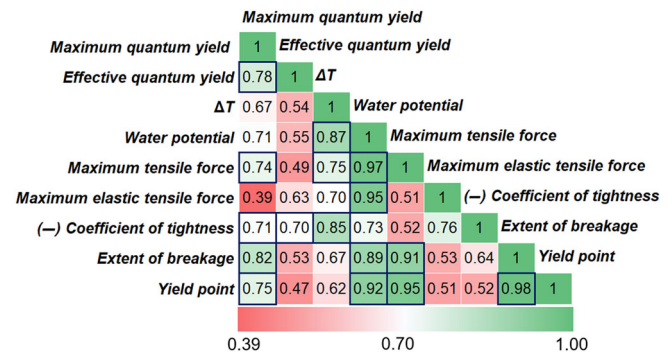


FIGURE 6 Pearson's linear correlation matrix for all variables. Numbers are the correlation value (r). Colour scale indicates more correlation in green and less correlation in red. Coefficient of tightness correlation is expressed multiplied by -1 . Blue edges indicate statistically significant correlation: p -value ≤ 0.05 .

tensile force (Figure 6). A PCA distributed samples along Principal Component 1 (PC1; accounting for 98.9% of total variance) in a DAG-dependant way (Figure S3A). After PCA, three groups of samples could be distinguished from the negative to the positive side of PC1: (1) initial stages of graft healing (1–4 DAG); (2) intermediate stages of graft healing (6–12 DAG) and (3) non-grafted and late stages of graft healing. PC2 contributed to further separate group 2 from groups 1 and 3. Water potential and ΔT were the variables with the highest contribution to PC1 and PC2 (Figure S3A).

4 | DISCUSSION

4.1 | Evolution of evaluated parameters during tomato graft healing

The study results showed the dynamics of several physical and physiological parameters during the tomato grafting process with specific healing conditions (Figure S3B) and are summarised in Figure 7.

PCA grouped initial, intermediate and late post-grafting times separately, indicating that the variables studied here are highly related to the graft healing process.

On the first DAG, all of the evaluated parameters, except quantum yields, decreased drastically with regard to non-grafted plants, showing the expected effects of grafting on the scion: water stress due to loss of xylem continuity, with the inherently reduced transpiration as a result of stomata closure (Hartmann et al., 2018; Martínez-Ballesta et al., 2010). Quantum yields also decreased but did not reach their minimum until 4 DAG. This delay may have occurred because the photosynthetic process is indirectly affected by water stress (via reduction of the CO_2 concentration in the mesophyll as a consequence of stomata closure), whereas water potential and transpiration are directly related to water availability (Martínez-Ballesta et al., 2010; Melnyk, 2017) (Figure 7).

Only ΔT and water potential, in a minor extent, started recovery at 4 DAG. In addition, xylem conductance showed that xylem transport was restored (poorly) from 4 DAG onwards. This might indicate

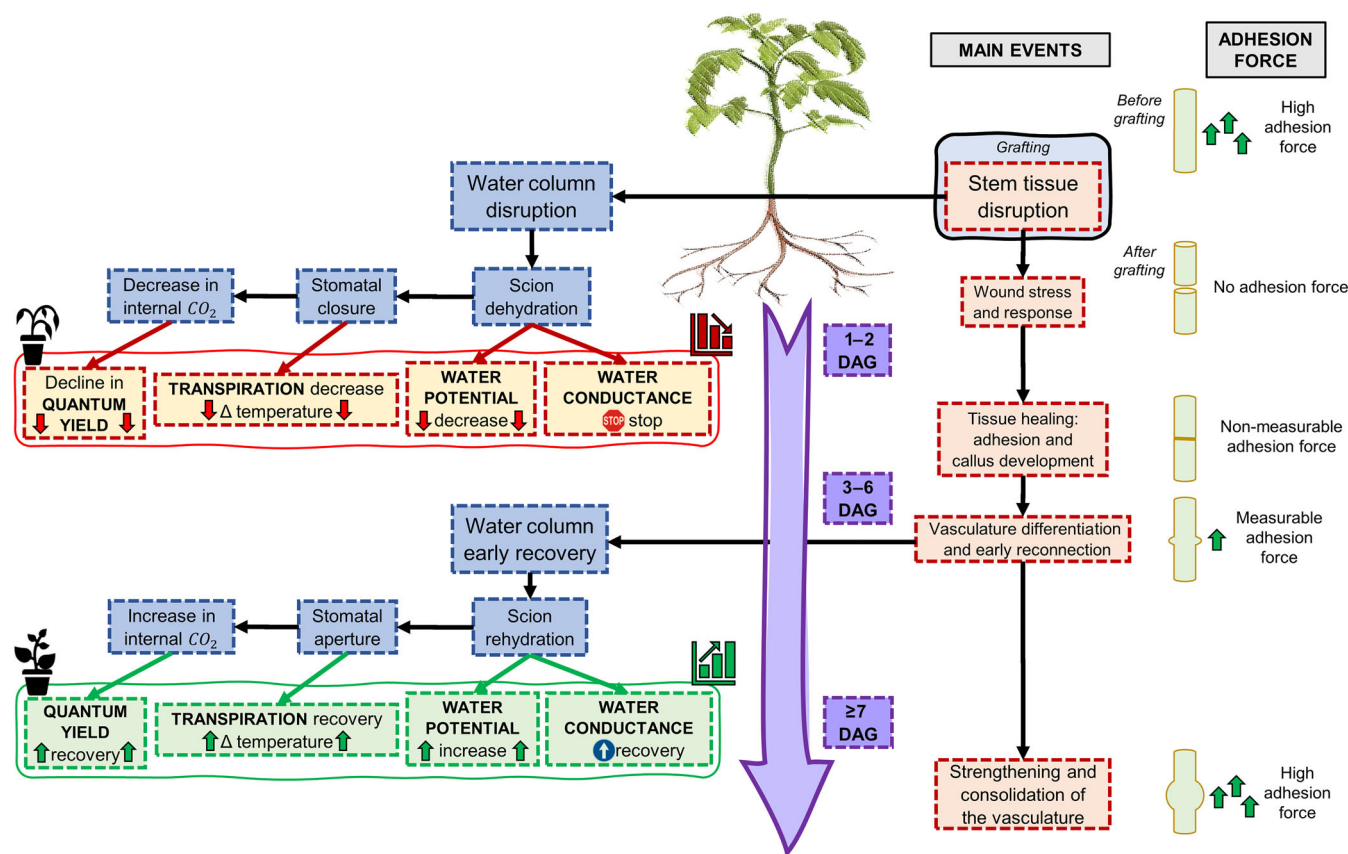


FIGURE 7 Scheme summarizing the graft dynamics with a particular focus on some of the changes in the physiological parameters studied here: quantum yield, transpiration, water potential and water conductance, together with adhesion force (maximum tensile force).

that transpiration recovered rapidly when water started to reach the scion. The recovery of water potential was prolonged, occurring between 4 and 12 DAG. However, the recovery of quantum yields and ΔT parameters was detected between the 4–6(8) DAG interval. The foregoing suggests that the interval corresponding to 4–6 DAG represents a critical threshold for the successful evolution of tomato grafts. In fact, we submit that if the graft union is not well established by this time, the scion may not overcome persistent water stress and the graft is likely to fail (Frey et al., 2021).

Water transfer to the scion depends on vasculature reconnection, at least by a few cells (Melnik et al., 2015). The evolution of transpiration and water potential parameters may be correlated with xylem connectivity. Transpiration changes could track early xylem connection and increased water potential, which appear to be well correlated with the amount of xylem that has reconnected. Previous histological studies showed complete xylem reconnection around 10 DAG (Frey et al., 2020). Here it is proposed that the earliest vascular reconnection takes place at approximately 4 DAG. Another study (Fan et al., 2015) claimed that vascular reconnection requires at least 7 days, but Fernández-García et al. (2004) reported functional water transport between 4 and 8 DAG, while Cui et al. (2021) indicated the 5–9 DAG interval, both of which are more in accordance with our results. However, healing conditions and the developmental stage of the plant must surely influence this process.

At 6 DAG, mechanical resistance parameters were measurable, but the union between scion and rootstock was still weak and only recovered values close to those of non-grafted controls at 16 DAG. In light of this finding, maximum tensile force seems to be correlated with the development of new vasculature after early reconnection (Lindsay et al., 1973; Moore, 1984).

4.2 | Effectiveness of thermography and quantum yield for monitoring graft healing

Thermography is a widely used technology in plant sciences research (Harrap et al., 2018). Nowadays, thermal images are being optimised for stress detection in crop fields, and they promise to become an essential tool in agriculture (Pineda et al., 2021). Thus, the state-of-the-art points to the use of thermography as a cutting-edge tool. Our study results support the potential application of thermography for inferring transpiration and monitoring graft healing. The thermographic method described here, based on determining leaf and environmental ΔT , has proven to be a good tool for monitoring tomato graft healing. Pearson's linear correlation matrix for all variables evidenced that ΔT correlated with physiological parameters that reliably indicate the development of the graft healing process: water potential and maximum tensile force. In addition, the high contribution of ΔT (inferred transpiration) to the PCs

further supports the hypothesis that this parameter is a good tool for graft monitoring. Furthermore, while water potential and maximum tensile force determinations are invasive and also rather complicated to perform in a short period of time, this method is simple, non-invasive and easy to perform in a short time. In research, some methods have been developed for monitoring vascular reconnection in grafts (Melnik et al., 2015; Wulf et al., 2020); however, they are equally cumbersome and invasive.

With regard to quantum yield measurements, in our study, the maximum quantum yield correlated better with the other parameters than the effective quantum yield. This finding fits well with the higher sensitivity to environmental stresses of photosystem II photochemistry compared to non-photochemical processes (Roháček, 2002), and therefore, only maximum quantum yield would seem to be an appropriate method to monitor graft healing, as it correlated well with mechanical resistance parameters. Calatayud et al. (2013) reported that maximum quantum yield is capable of identifying compatibility problems in melon grafts. In addition, the use of chlorophyll fluorescence parameters has already been used to monitor water stress (Calatayud et al., 2006). Furthermore, the maximum quantum yield has been applied to evaluate different plant stresses, such as salt stress, for example, in tomato plants (Shin et al., 2020).

In conclusion, the clear distribution of physical and physiological parameters into three temporal groups is evidence of the evolution over time of these variables and implies that they are highly related to the graft healing process, supporting the potential use of some of these variables to monitor the grafting process. Monitoring grafting progress using thermography and/or maximum quantum yield measurements could be useful for companies interested in acquiring affordable and effective control over grafting plants to efficiently adjust healing chamber conditions. Moreover, these methods could serve as early detection markers of graft failure and could play a role in transforming the horticulture industry by reducing costs, in time and money, for grafting operators. Scale-up of the technique presented here has high potential to improve the yield of grafted tomato (and analogous crops). However, to achieve this, several recommendations should be taken into account: to be effective, thermography for monitoring transpiration requires that the environmental conditions should be controlled to the greatest extent possible, trying to take the measurements at the same hour of the day and avoiding the effect of wind or variations in light or humidity (Poirier-Pocovi & Bailey, 2020; Savvides et al., 2022). If applying this method to plants grown in a greenhouse, then thermography should be used in sunny conditions and on plants in well-watered substrates (Poirier-Pocovi & Bailey, 2020; Violet-Chabrand & Lawson, 2020). It is advisable to standardise leaf temperature measurements, always photographing perpendicular to the leaf and at the same distance, and introducing reference temperatures to control for sensitivity to ambient conditions such as radiation, air temperature, humidity, etc. (Jones et al., 2009; Savvides et al., 2022; Violet-Chabrand & Lawson, 2020). Finally, these techniques should be specified for each grafted crop, taking into account that their physiological responses to stresses, water or radiation requirements or photosynthetic efficiencies, to cite some examples, may differ (Costa et al., 2013; Jones et al., 2009).

AUTHOR CONTRIBUTIONS

Antonio Encina and José Luis Acebes conceived and designed the research, supervised the experiments, analysed the data and prepared the final version of the manuscript. Carlos Frey and Andrés Hernández-Barriuso conducted the experiments, analysed the data and wrote the draft of the manuscript. All authors have read and agreed to the published version of the manuscript. Carlos Frey and Andrés Hernández-Barriuso contributed equally to this work.

ACKNOWLEDGMENTS

Authors acknowledge Dr. Reyes Tárrega and Dr. Alicia Quirós for their advice in the statistical treatment of the data, Denise Phelps for her English language revisions, and Fabrication and 3D Impression Service of Universidad de León for their advice on the use of the universal tensile testing system use.

FUNDING INFORMATION

This research was funded by Universidad de León. C.F. acknowledges the PhD grant from the FPU program of the Spanish Universities Ministry (FPU18/04934).

CONFLICT OF INTEREST STATEMENT

The authors declare no competing interests.

DATA AVAILABILITY STATEMENT

The data that support the findings of this study are available from the corresponding author upon reasonable request.

ORCID

Carlos Frey  <https://orcid.org/0000-0002-0369-5536>

Antonio Encina  <https://orcid.org/0000-0002-1559-1136>

José Luis Acebes  <https://orcid.org/0000-0002-0960-085X>

REFERENCES

- Bletsos, F. & Olympios, C. (2008) Rootstocks and grafting of tomatoes, peppers and eggplants for soil-borne disease resistance, improved yield and quality. *Eur J Plant Sci Biotechnol*, 2, 62–73.
- Calatayud, A., Roca, R. & Martínez, P.F. (2006) Spatial-temporal variations in rose leaves under water stress conditions studied by chlorophyll fluorescence imaging. *Plant Physiol Biochem*, 44, 564–573.
- Calatayud, A., San Bautista, A., Pasqual, B., Maroto, J.V. & López-Galarza, S. (2013) Use of chlorophyll fluorescence imaging as diagnostic technique to predict compatibility in melon graft. *Sci Hortic*, 149, 13–18.
- Colla, G., Rouphael, Y., Leonardi, C. & Bie, Z. (2010) Role of grafting in vegetable crops grown under saline conditions. *Sci Hortic*, 127(2), 147–155.
- Costa, J.M., Grant, O.M. & Chaves, M.M. (2013) Thermography to explore plant-environment interactions. *J Exp Bot*, 64(13), 3937–3949.
- Cui, Q., Xie, L., Dong, C., Gao, L. & Shang, Q. (2021) Stage-specific events in tomato graft formation and the regulatory effects of auxin and cytokinin. *Plant Sci*, 304, 110803.
- Fan, J., Yang, R., Li, X., Zhao, W., Zhao, F. & Wang, S. (2015) The processes of graft union formation in tomato. *Hortic Environ Biotechnol*, 56(5), 569–574.
- FAO. (2021) The State of Food and Agriculture 2021. Making agrifood systems more resilient to shocks and stresses. FAO. <https://doi.org/10.4060/cb4476en>

- Fernández-García, N., Carvajal, M. & Olmos, E. (2004) Graft union formation in tomato plants: peroxidase and catalase involvement. *Ann Bot*, 93(1), 53–60.
- Frey, C., Acebes, J.L., Encina, A. & Álvarez, R. (2020) Histological changes associated with the graft union development in tomato. *Plants*, 9(11), 1479.
- Frey, C., Álvarez, R., Encina, A. & Acebes, J.L. (2021) Tomato graft union failure is associated with alterations in tissue development and the onset of cell wall defense responses. *Agronomy*, 11(6), 1197.
- Frey, C., Manga-Robles, A., Acebes, J.L. & Encina, A. (2022) The graft framework: quantitative changes in cell wall matrix polysaccharides throughout the tomato graft union formation. *Carbohydr Polym*, 276, 118781.
- Frey, C., Martínez-Romera, N., Encina, A. & Acebes, J.L. (2023) Immunohistochemical dynamics of cell wall matrix polymers during tomato autograft healing. *Plant Mol Biol*. Available from: <https://doi.org/10.1007/s11103-023-01351-7>
- Gosa, S.C., Koch, A., Shenhar, I., Hirschberg, J., Zamira, D. & Moshelion, M. (2022) The potential of dynamic physiological traits in young tomato plants to predict field-yield performance. *Plant Sci*, 315, 111122.
- Harrap, M.J.M., de Ibarra, N.H., Whitney, H.M. & Rands, S.A. (2018) Reporting of thermography parameters in biology: a systematic review of thermal imaging literature. *R Soc Open Sci*, 5, 181281.
- Hartmann, H.T., Kester, D.E., Davies, F.T. & Geneve, R.L. (2018) *Hartmann & Kester's plant propagation principles and practices*, 9th edition. Harlow: Pearson.
- Hoagland, D.R. & Arnon, D.I. (1938) The water culture method for growing plants without soil. California Agr Exp Sta Cir No 347, 32. Berkeley, California: College of Agriculture, University of California.
- Jeffree, A.C.E. & Yeoman, M.M. (1983) Development of intercellular connections between opposing cells in a graft union. *New Phytol*, 93(4), 491–509.
- Jones, H.D. (2004) Application of thermal imaging and infrared sensing in plant physiology and ecophysiology. *Adv Bot Res*, 41, 107–163.
- Jones, H.G., Serraj, R., Loveys, B.R., Xiong, L., Wheaton, A. & Price, A.H. (2009) Thermal infrared imaging of crop canopies for the remote diagnosis and quantification of plant responses to water stress in the field. *Funct Plant Biol*, 36, 978–979.
- Lindsay, D.W., Yeoman, M.M. & Brown, R. (1973) An analysis of the development of the graft union in *Lycopersicon esculentum*. *Ann Bot*, 38(3), 639–646.
- Louws, F.J., Rivard, C.L. & Kubota, C. (2010) Grafting fruiting vegetables to manage soilborne pathogens, foliar pathogens, arthropods and weeds. *Sci Hortic*, 127(2), 127–146.
- Maes, W.H. & Steppe, K. (2012) Estimating evapotranspiration and drought stress with ground-based thermal remote sensing in agriculture: A review. *J Exp Bot*, 63, 4671–4712.
- Martínez-Ballesta, M.C., Alcaraz-López, C., Muries, B., Mota-Cadenas, C. & Carvajal, M. (2010) Physiological aspects of rootstock-scion interactions. *Sci Hortic*, 127(2), 112–118.
- Mauro, R.P., Agnello, M., Distefano, M., Sabatino, L., San Bautista Primo, A., Leonardi, C. et al. (2020) Chlorophyll fluorescence, photosynthesis and growth of tomato plants as affected by long-term oxygen root zone deprivation and grafting. *Agronomy*, 10(1), 137.
- Melcher, P.J., Holbrook, N.M., Burns, M.J., Zwieniecki, M.A., Cobb, A.R., Brodribb, T.J. et al. (2012) Measurements of stem xylem hydraulic conductivity in the laboratory and field. *Methods Ecol Evol*, 3, 685–694.
- Melnyk, C.W. (2017) Plant grafting: insights into tissue regeneration. *Regeneration*, 4(1), 3–14.
- Melnyk, C.W., Schuster, C., Leyser, O. & Meyerowitz, E.M. (2015) A developmental framework for graft formation and vascular reconnection in *Arabidopsis thaliana*. *Curr Biol*, 25(10), 1306–1318.
- Moore, R. (1984) Graft formation in *Solanum pennellii* (Solanaceae). *Plant Cell Rep*, 3(5), 172–175.
- Notaguchi, M., Kurotani, K.I., Sato, Y., Tabata, R., Kawakatsu, Y., Okayasu, K. et al. (2020) Cell-cell adhesion in plant grafting is facilitated by β -1,4-glucanases. *Science*, 369(6504), 698–702.
- Oda, M., Maruyama, M. & Mori, G. (2005) Water transfer at graft union of tomato plants grafted onto *Solanum* rootstocks. *J Jpn Soc Hortic Sci*, 74(6), 458–463.
- Pina, A. & Errea, P. (2005) A review of new advances in mechanism of graft compatibility-incompatibility. *Sci Hortic*, 106(1), 1–11.
- Pineda, M., Barón, M. & Pérez-Bueno, M.L. (2021) Thermal imaging for plant stress detection and phenotyping. *Remote Sens*, 13, 68.
- Poirier-Pocovi, M. & Bailey, B.N. (2020) Sensitivity analysis of four crop water stress indices to ambient environmental conditions and stomatal conductance. *Sci Hortic*, 259, 108825.
- Reeves, G., Tripathi, A., Singh, P., Jones, M.R.W., Nanda, A.K., Musseau, C. et al. (2022) Monocotyledonous plants graft at the embryonic root-shoot interface. *Nature*, 602, 280–286.
- Roháček, K. (2002) Chlorophyll fluorescence parameters: the definitions, photosynthetic meaning, and mutual relationships. *Photosynthetica*, 40(1), 13–29.
- Savvides, A.M., Velez-Ramirez, A.I. & Fotopoulos, V. (2022) Challenging the water stress index concept: thermographic assessment of Arabidopsis transpiration. *Physiol Plant*, 174, e13762.
- Shin, Y.K., Bhandari, S.R., Cho, M.C. & Lee, J.G. (2020) Evaluation of chlorophyll fluorescence parameters and proline content in tomato seedlings grown under different salt stress conditions. *Hortic Environ Biotechnol*, 61, 433–443.
- Sun, L., Zhao, W., Jiang, M., Yang, R., Sun, X., Wang, J. et al. (2021) Rootstock screening for greenhouse tomato production under a coconut coir cultivation system. *Chil J Agric Res*, 81(2), 202–209.
- Thomas, H., Van der Broeck, L., Spurney, R., Sozzani, R. & Frank, M. (2022) Gene regulatory networks for compatible versus incompatible grafts identify a role for SIWOX4 during junction formation. *Plant Cell*, 34, 535–556.
- Torii, T., Kasiwazaki, M., Okamoto, T. & Kitani, O. (1992) Evaluation of graft-take using a thermal camera. *Acta Hortic*, 319, 631–634.
- Violet-Chabrand, S. & Lawson, T. (2020) Thermography methods to assess stomatal behaviour in a dynamic environment. *J Exp Bot*, 71(7), 2329–2338.
- Wulf, K.E., Reid, J.B. & Foo, E. (2020) What drives interspecies graft union success? Exploring the role of phylogenetic relatedness and stem anatomy. *Physiol Plant*, 170, 132–147.
- Yang, S., Xiang, G., Zhang, S. & Lou, C. (1993) Electrical resistance as a measure of graft union. *J Plant Physiol*, 141(1), 98–104.
- Zhang, A., Matsuoka, K., Kareem, A., Robert, M., Roszak, P., Blob, B. et al. (2022) Cell-wall damage activates DOF transcription to promote wound healing and tissue regeneration in *Arabidopsis thaliana*. *Curr Biol*, 32(9), 1883–1894.

SUPPORTING INFORMATION

Additional supporting information can be found online in the Supporting Information section at the end of this article.

How to cite this article: Frey, C., Hernández-Barriuso, A., Encina, A. & Acebes, J.L. (2023) Non-invasive monitoring of tomato graft dynamics using thermography and fluorescence quantum yields measurements. *Physiologia Plantarum*, 175(3), e13935. Available from: <https://doi.org/10.1111/ppl.13935>